Mixed-State Wetting and Wetting Transitions on Laser Surface Engineered Polymeric Materials

Waugh, D., Lawrence, J., Langer, N. & Bidault, S.

Original citation:
Waugh, D, Lawrence, J, Langer, N & Bidault, S 2018, 'Mixed-State Wetting and Wetting Transitions on Laser Surface Engineered Polymeric Materials' International Journal of Wettability Science and Technology, vol. 1, no. 1, pp. 63-84.

ISSN 2473-5035
ESSN 2473-5043

Publisher: Old City Publishing

Int. Journ. of Wettability Science and Technology, Vol. 1, pp. 63–84
Reprints available directly from the publisher.
Photocopying permitted by license only.

Mixed-State Wetting and Wetting Transitions on Laser Surface Engineered Polymeric Materials

D. G. WAUGH*[1], J. LAWRENCE[1], N. LANGER[2] AND S. BIDAULT[2]

[1]*School of Mechanical, Aerospace and Automotive Engineering, Faculty of Engineering, Environment and Computing, Coventry University, Gulson Road, Coventry, CV1 2JH, UK*
[2]*DataPhysics Instruments GmbH, Raiffeisenstraße 34, 70794 Filderstadt, Germany*

Currently, there is a significant amount of work in the field of wettability science to try and better understand wetting transitions and subsequent developments of mixed-state wetting regimes. This is of extreme importance as this knowledge will have significant impact in those industries and academic fields which rely heavily on adhesion science. This work details the implementation of CO_2 lasers to surface engineer polymeric materials, poly(methyl methacrylate) (PMMA) and polyamide 6,6 (nylon 6,6), to bring about and gain a further understanding of the wetting nature of laser surface engineered polymeric materials. With the laser, the surface roughness (Ra) was dramatically increased by up to 4.5 μm in comparison to the as-received sample (AR). It was determined for all samples that the polar component had a strong inverse relationship with the contact angle, θ. For the laser surface engineered polymers a modest increase in θ indicated a possible formation of a mixed-state wetting regime, highlighting the influence of laser-modified surface topography on θ. The polar component and surface pattern were found to be the most dominant parameters governing the wettability characteristics of the laser-surface-modified polymeric materials. The latest state-of-the-art knowledge and understanding of wetting transitions and mixed-state wetting regimes with specific regard to roughened laser surface engineered polymeric materials is discussed identifying significant wettability knowledge and theories.

Keywords: Laser surface engineering, PMMA, nylon 6,6, polymers, wetting transitions, mixed-state wetting.

*Corresponding author's e-mail: david.waugh@coventry.ac.uk

1 INTRODUCTION

Wettability science is fast becoming a mainstream subject field for industrialists and academics alike, being applied to a wide range of adhesion applications [1-4] such as biomedical applications [5-9] and coating technologies [2,10,11]. As a direct consequence of this rapid expansion of interest, many working in the field are striving for a full and complete understanding of liquid material interfaces expanding on the current understanding relating to Wenzel wetting regimes [12] and Cassie-Baxter wetting regimes [13]. This is owed to the fact that, in some instances, these theories do not correspond to experimental observations with wetting transitions not being properly accounted for. In fact, a recent review of the laser surface-modified wettability literature [14] enabled one to realise that laser modified wettability characteristics of materials are not being reported uniformly, giving rise to a disjointed scientific community approach. Within the wettability science community, though, there has been an exponential growth in the studies of wetting regimes and the transitions between these various regimes over the past ten years [12,15-18]. With these works in mind, it is crucial for the surface engineering community to take significant note and collaborate with colleagues working in the field of wettability science to further understand the wetting regimes taking place on surface engineered materials. This thought is borne from the understanding and knowledge that, through surface engineering, a hydrophilic surface can give rise to a form of mixed state wetting regime due to the modifications brought about to the surface roughness and surface topography [15,18-20].

With an increased need from industry for cheaper and easier to manufacture materials, polymers have increased in application [19,21-23], covering numerous industries and fields over the last ten years. Considering the adhesive properties of polymeric materials, generally most polymeric materials have insufficient wettability and adhesion characteristics which means they tend to have inferior bond qualities compared to other material types [24]. With the increased interest in polymeric materials, researchers have started to consider using surface engineering technologies to manipulate the surface of polymeric materials to enhance that the wettability characteristics and subsequently the adhesion properties of these materials. This has especially been evidenced with biomedical applications in which it has been shown that polymeric biomaterials have adequate bulk properties but severely lack the necessary surface properties to give rise to adequate cell response [25,26]. With this in mind, for the biomedical and healthcare industries to take up polymeric materials, it is critical for researchers to find a way to modify the surface of a polymeric material to enhance and gain a better understanding of the surface adhesive properties. This and having a thorough in-depth understanding of how the arising wetting regimes, and the transitions between them, impact upon the adhesive properties of the polymeric materials is crucial for

having a full and complete understanding of how the surface properties can be modified through surface engineering for a specific application.

Along with the increased uptake of polymeric materials, there has been a large number of techniques developed and enhanced which can be used to modify the surfaces of materials. Laser surface engineering offers a number of benefits including flexibility, accuracy and negligible bulk modification [27-29]. Utilizing lasers for surface engineering has also been seen to be an attractive method in a number of industries as they enable a relatively clean processing emphasizing the reducing the need for post-processing, ultimately reducing manufacturing running costs. In the literature, it can be seen that there has been a considerable amount of work carried out showing that the wettability characteristics and adhesion properties of polymeric materials can be modified by means of laser surface engineering [6,19,30-33]. However, what is extremely apparent is the lack of conformity in the approach to how the wettability science study is reported. On account of this, there is a lack of deep understanding into how the liquid-surface interface reacts to these laser-induced surface modifications.

The work within this manuscript shows how laser surface engineering can be employed to modify the surface characteristics of polymeric materials, offering potential solutions and progression routes to understanding the wetting regimes and wetting transitions which arise on laser surface engineered polymeric materials.

2 EXPERIMENTAL DETAILS

2.1 Material Specifications

Poly(methyl methacrylate) (PMMA) (T_m = 160°C/433 K) was sourced in 150×150 mm^2 sheets with a thickness of 5 mm (Goodfellow Cambridge, Ltd). Polyamide 6,6 (nylon 6,6) (T_m = 267°C/540 K) was sourced in 100×100 mm^2 sheets with a thickness of 5 mm (Goodfellow Cambridge, Ltd). A 1kW continuous wave (cw) CO_2 laser (Everlase S48; Coherent, Ltd) was used to obtain a conveniently sized sample for experimentation. That is, the as-received sheets were cut into 30 mm diameter discs. It should be noted that there was no discernible heat affected zone (HAZ) observed under optical microscopic examination.

2.2 Laser Surface Engineering Approach

In order to generate the required marking pattern with the 10.6 μm Synrad cw 10W CO_2 laser system Synrad Winmark software version 2.1.0, build 3468 was used. The samples were placed into the laser system onto a stage and held in place using a bracket. The surface of the sample was fixed at 250 mm away from the output facet of the laser to obtain focus and the system utilized a galvanometer scanner to scan the 95 μm spot size beam. It should be noted

that the target material and laser system was held in a laser safety cabinet in which the ambient gas was air and an extraction system was used to remove any fumes produced during laser processing.

There were four patterns induced onto the surfaces of the samples. These were trenches with 50 μm spacing (T50), hatch with 50 μm spacing (H50), trenches with 100 μm spacing (T100) and hatch with 100 μm spacing (H100). In addition, an as-received control sample was used (AR). It should be noticed that all PMMA sample codes are preceded by the letter 'P' and the nylon 6,6 samples are preceded with the letter 'N'. For each of the irradiated patterns the laser power was set to 70% (7 W) operating at 600 $mm_s^{-1.}$

2.3 Analytical Technique Procedures

After laser surface engineering, the samples were analysed using an optical microscope (Flash 200 Smartscope; OGP, Ltd) to obtain optical micrographs of the samples. Also, surface profiles of the samples were determined using a white light interferometer (WLI) (NewView 500; Zygo, Ltd) with MetroPro and TalyMap Gold Software. The Zygo WLI was setup using a ×10 Mirau lens with a zoom of ×0.5 and working distance of 7.6 mm. This system also allowed Sa and Ra roughness parameters to be determined for each sample.

The samples were ultrasonically cleaned in isoproponal (Fisher Scientific Ltd., UK) for 3 minutes at room temperature before using a sessile drop device (OCA20; Dataphysics Instruments, GmbH) to determine the wettability characteristics. This was to allow for a relatively clean surface prior to any contact angle measurements being taken. To ensure that the sample surfaces were dry, a specimen dryer (Metaserv, UK) was utilized to blow ambient air across the samples. To obtain recent advancing contact angles, θ, using triply distilled water and the recent advancing contact angles, θ, using diodomethane for each sample the sessile drop device was used with relevant software (SCA20; Dataphysics Instruments, GmbH). The advancing θ for each liquid was measured by dispensing a 5 μl volume, at a dispensing rate of 2μl/s, onto the sample surfaces. Liquid (2 μl at 2 μ/s) was then added to the droplet at 1 minute intervals until the triple line [34] advanced along the surface. Once the triple line advanced, the advancing θ was measured and recorded and these steps were repeated to measure multiple advancing θ on each sample. It should be noted here that ten contact angles, using two droplets, in each instance was recorded to achieve a mean θ for each liquid and surface. By utilizing the advancing θ for the two liquids with the software an Owens, Wendt, Rabel and Kaeble (OWRK) plot was produced to determine the apparent dispersive component, $\gamma^{D,}$ the apparent polar component, γP, and the total apparent surface free energy, γT, of the samples. For the two reference liquids the SCA20 software used the Ström et al. [35] literature values to calculate γT of the samples. On account of the universal applicability of the OWRK data evaluation approach for determining the dispersive and polar

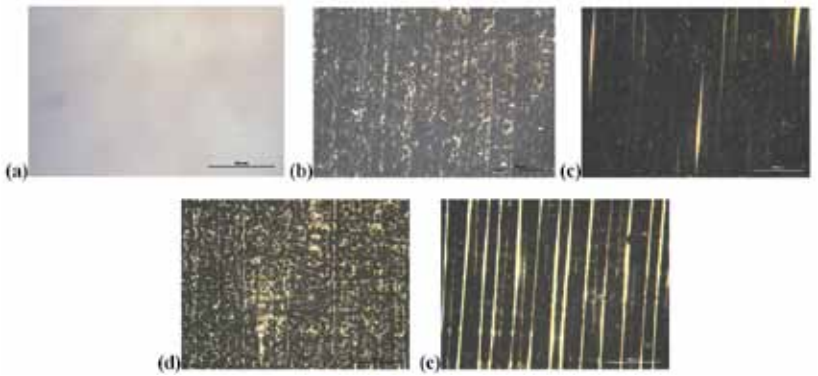

FIGURE 1
Optical micrographs of PMMA samples: a) as-received (PAR), b) 50 μm trench (PT50), c) 100 μm trench (PT100), d) 50 μm hatch (PH50) and e) 100 μm hatch (PH100).

components of the free surface energy [36], a minimum of two liquids were chosen. For this research, the liquids chosen were triply distilled water and diodomethane, meeting the OWRK evaluation requirements of having one liquid with a dominant polar component and the other with a dominant dispersive component.

All samples were sputter coated with Au to attain adequate conductance and analysed using scanning electron microscopy (SEM). In addition, prior to coating for SEM, X-ray photoelectron spectroscopy (XPS) analysis was carried out to allow any surface modifications in terms of chemical composition due to the laser irradiation to be revealed. Further details pertaining to the SEM and XPS set-up can be found in [24,37].

3 RESULTS AND DISCUSSION

3.1 Laser Surface Modified Topography

It is evident from the micrographs, shown in Figure 1, that the laser induced patterns (see Figures 1(b) – 1(e)) gave rise to considerable melting of the PMMA surface. This arises due to the fact that the 10.6 μm laser beam interaction with the PMMA surface is a thermolytical process owed to the laser coupling into the material in the form of bond and lattice vibrations. Figure 1 also highlights, qualitatively, the major differences between induced surface patterns as well as between the as-received PMMA sample (sample PAR). It can be seen that the trench and hatch patterns with 50 μm spacing (see Figures 1(b) and (d)) gave rise to considerably more melting in comparison to that of the trench and hatch patterns with 100 μm spacing (see Figures 1(c) and (e)). This was a result of the spot size of the laser beam at the surface of the material was 95 μm which gave rise to the pattern overlapping on the 50 μm spaced samples, causing areas to re-melt

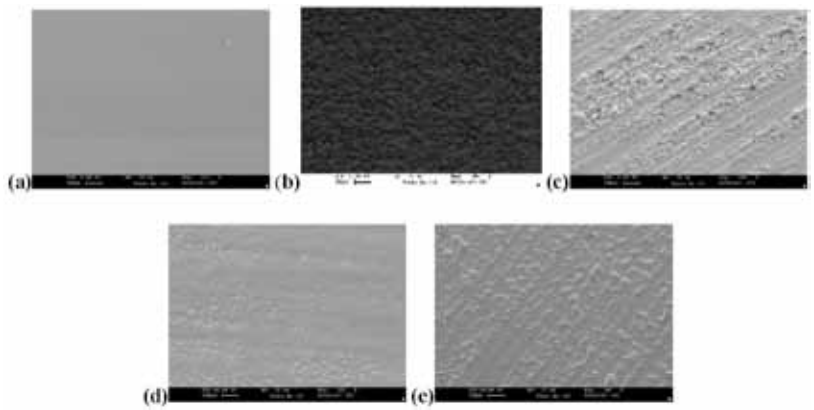

FIGURE 2
SEM micrographs of PMMA samples: (a) as-received (PAR), (b) 50 μm trench (PT50), (c) 100 μm trench (PT100), (d) 50 μm hatch (PH50), (e) 100 μm hatch (PH100).

and re-solidify. It is also necessary to note here that the hatch patterns (samples PH50 and PH100) shown in Figure 1(d) and (e) appear to have had the topographical hatch more prominent in the y-axis in comparison to the x-axis. This is on account of the way in which the laser interacted with the material as the laser scanned the pattern across the material surface. In order to confirm what was observed through optical microscopic analysis the samples were also studied by obtaining SEM images which can be seen in Figure 2.

Like the optical microscopy analysis, SEM analysis of the samples (see Figure 2) showed that the surface of the laser patterned PMMA samples had been modified in comparison to that of the as-received sample. It was also interesting to see that SEM images of the 50 μm spaced patterns (see Figures 2 (b) and (d)) indicated that the intended topographical pattern had been slightly distorted due to the large amount of surface melting that appears to have taken place. Furthermore, from Figure 2 (d) it was suggested that the 50 μm hatch pattern (sample PH50) gave rise to a smoother surface in comparison to the other laser patterned samples which can be accounted to the surface melting and re-melting. Whereas SEM images of the other laser patterned samples (see Figure 2 (a) – (c) and (e)) imply that, owed to the surface melting and re-solidifying, protrusions away from the surface formed resulting in a considerable increase in surface roughness.

In order to obtain the roughness parameters, quantatively, WLI was employed which allowed for continuous axonometric images and surface profile extractions to be generated. This allowed a 3-D profile of each of the sample surfaces to be obtained. Figure 3 shows the 3D profile for the as-received PMMA reference sample (sample PAR).

The 3D surface profile for the as-received PMMA sample (PAR) shown in Figure 3 revealed that in relation to the laser patterned samples the surface of the PAR sample was markedly smoother with peak heights of up to 0.4 μm

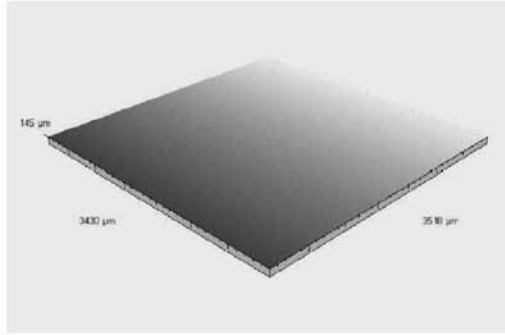

FIGURE 3
Continuous axonometric 3D profile for the as-received sample (AR).

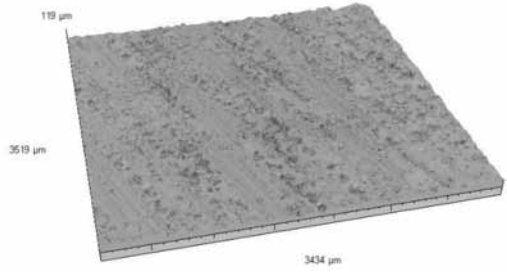

FIGURE 4
Continuous axonometric 3D profile for laser induced 50 µm trench pattern (PT50).

leading to Sa and Ra values of 0.04 and 0.03 µm, respectively. This is contrasted with the laser patterned samples (see Figure 4 to 7).

Figure 4 shows the resulting 3D surface profile from the WLI analysis of the 50 µm trench patterned sample. From this, it can be seen that the surface topography for the 50 µm trench sample was considerably rougher in comparison to the as-received sample (sample PAR) with peak heights of up to 10 µm and roughness values of 2.66 and 1.63 µm for Sa and Ra, respectively. Similar values with an Sa of 2.65 µm, an Ra of 1.43 µm and peak heights ranging between 10 and 15 µm, were also observed for the sample laser patterned using 100 µm trenches (see Figure 5).

It is evident from both Figures 4 and 5 that a significant amount of surface melting had taken place as a direct result of the laser-material interaction. This melting and re-solidification can be seen to eliminate some of the intended periodic pattern induced by the laser processing. This can also be seen in Figures 6 and 7 which depict the results from the WLI analysis of the 50 and 100 µm hatch patterns, respectively. The elimination of the intended periodic pattern is highly demonstrated with the observed results of the 50

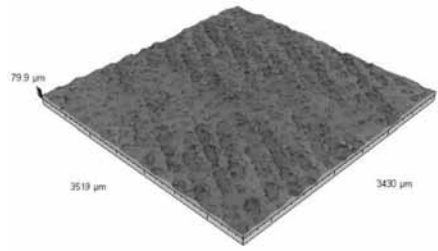

FIGURE 5
Continuous axonometric 3D profile for laser induced 100 µm trench pattern (PT100).

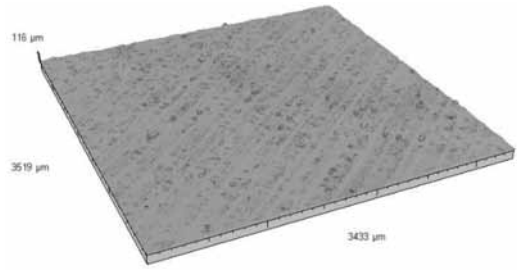

FIGURE 6
Continuous axonometric 3D profile for laser induced 50 µm hatch pattern (PH50).

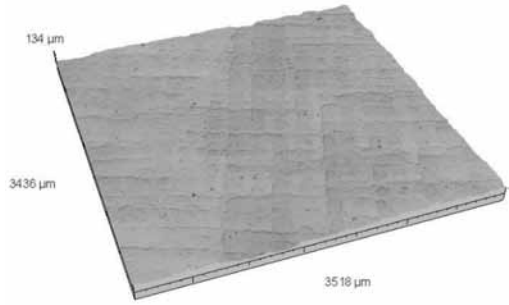

FIGURE 7
Continuous axonometric 3D profile for laser induced 100 µm hatch pattern (PH100).

µm hatch pattern (see Figure 6) as only one axis is well defined for the pattern. As discussed previously this is owed to the way in which the material interacts with the PMMA surface. That is, for the hatch patterns, the laser system scanned one axis first and then another giving rise to the pattern induced on the first scan being eradicated due to the melting and re-solidification arising from the second scan.

TABLE 1
A summary of the PMMA samples results along with their characteristic contact angle with triply distilled water.

Sample	Sa (μm)	Ra (μm)	γ^P (mJm^{-2})	γ^D (mJm^{-2})	γ^T (mJm^{-2})	Surface Oxygen Content (%at.)	Contact Angle (°)
(PAR)	0.04	0.03	3.46	26.95	30.40	15.5±0.31	85.6 ±2.6
(PT50)	2.66	1.63	5.13	35.08	40.21	17.3±0.35	75.2 ±1.9
(PT100)	2.65	1.43	0.20	36.23	36.42	19.9±0.40	94.2 ±4.1
(PH50)	3.16	0.87	8.27	33.93	42.21	18.0±0.36	69.1 ±1.9
(PH100)	1.61	0.98	1.70	37.08	38.78	17.8±0.35	84.4 ±3.1

Even though the periodic hatch pattern was somewhat eradicated during the laser processing it can be seen that the surface topography was also ultimately modified in comparison to the as-received sample (sample PAR). It was found that the 50 μm hatch pattern gave rise to peak heights to a maximum of approximately 12 μm with the surface roughness parameters being somewhat different to the other laser patterned samples with an Sa of 3.16 μm and Ra of 0.87 (see Table 1). This difference is born from the large difference between the Sa and Ra values for this sample; however, this can be seen to be of significance due to the fact that the Ra value could have been taken along a smoother section of the surface which had undergone melting and re-solidification. This could have resulted in a dramatic reduction of the Ra parameter. In contrast, the Sa parameter takes in to account the whole area of the 3D surface profile and, as such, both rougher and smoother sections of the surface would be taken in to account. In this instance, therefore, it can be argued that the Sa parameter value is more descriptive of the sample surface.

Figure 7 shows that, as a result of the laser induced hatch pattern, the surface appears smoother in comparison to the other laser patterned samples. This is owed to melting and re-solidification as the laser beam was scanned across the surface. It should also be noted that compared to Figure 6, Figure 7 shows that the 100 μm hatch pattern (PH100) kept more of the natural periodicity of the intended pattern owed to the fact that the larger dimensions allow for the scanned pattern to not overlap itself.

The smoothness observed from the 100 μm hatch pattern (see Figure 7) was confirmed by obtaining Sa and Ra values of 1.61 and 0.98 μm, respectively. Like the 50 μm hatch pattern shown in Figure 6, the Ra parameter can be seen to be lower due to this parameter taking into account a single line profile rather than including the whole area which is incorporated in determining the Sa parameter. It was also observed that for the 100 μm hatch pattern peak heights of up to 15 μm were obtained. This result coincides with the peak height values arising from the other laser patterned samples.

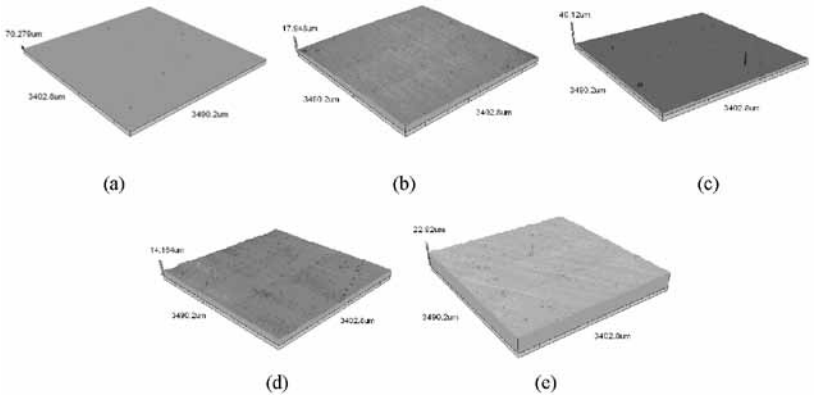

FIGURE 8
Continuous axonometric images for (a) as-received (NAR) (b) CT50 (b) CT100 (d) CH50 and (d) CH100.

Through Figures 8 and 9 it can be deduced that the laser patterned nylon 6,6 samples had considerably rougher surfaces with the largest peak heights being of the order of 2 μm for the laser patterned samples in contrast to the as-received sample (see Figure 8) which had peaks heights of up to 0.2 μm. On account of the increase in peak heights over the CO_2 laser-patterned samples the surface roughness (see Table 2) increased considerably with the largest Sa of 0.4 μm being achieved with the 50 μm hatch sample (NH50) and largest Ra of 0.2 μm for the 100 μm trench sample (NT100). It is given in Table 2 that the patterned samples with scan dimensions of 50 μm (samples NT50 and NH50) have larger Sa roughness values when compared to the samples patterned with 100 μm scan dimensions (samples NT100 and NH100). This can be attributed to the fact that the 50 μm scan dimensions irradiated more of the sample giving rise to an increase of mass being melted and re-solidified. Also, it can be seen from the Table 2 that the roughness for the hatch patterns had decreased in comparison to the trench patterns. This can be explained by the laser re-melting sections of the nylon 6,6 surface owed to the scanning process of the system. By re-melting these sections the material could then have re-solified into a smoother surface topography.

3.2 Laser Surface Modified Wettability

Table 1 gives a summary of the topography, surface oxygen content and wettability data obtained for each of the PMMA samples studied. In terms of wettability it can be seen that the as-received PMMA (sample PAR) was predominantly hydrophilic on account of the characteristic contact angle being less than 90°. In comparison to the as-received sample (PAR) there was a significant reduction in contact angle for both the 50 μm trench and hatch

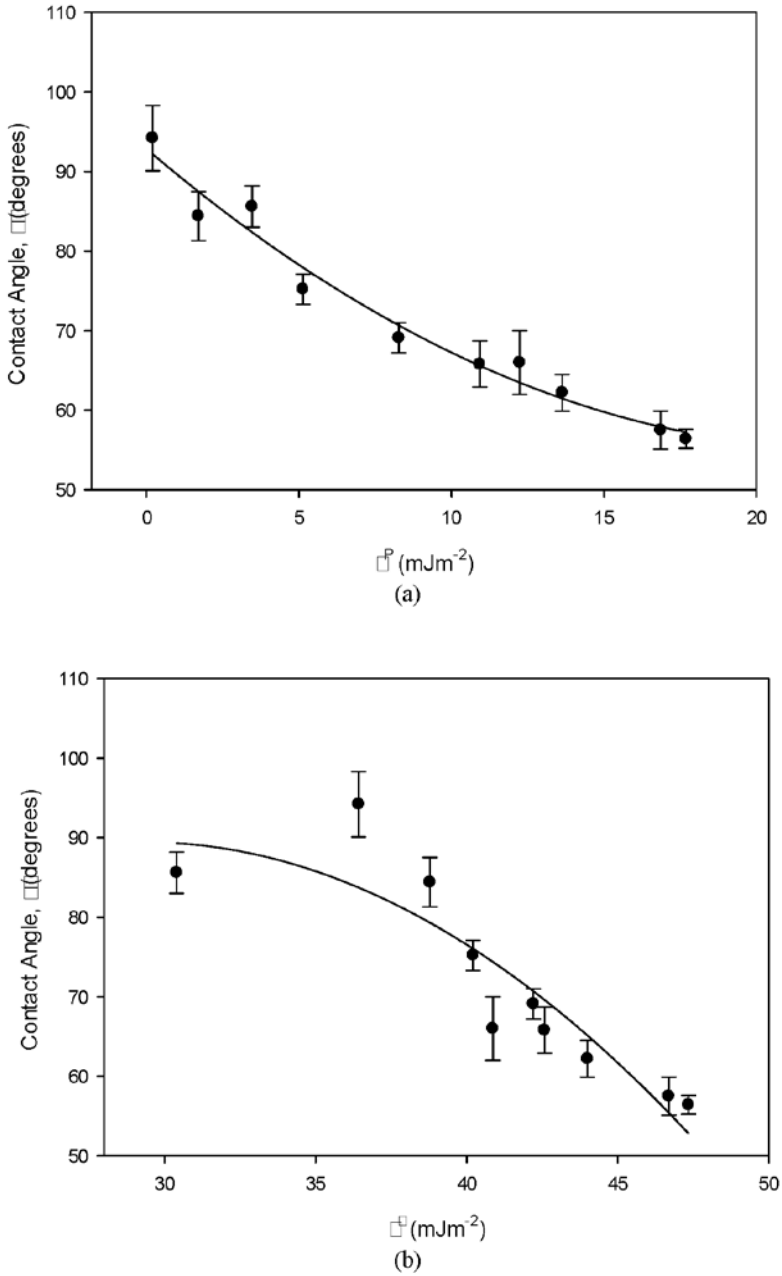

FIGURE 9
Graphs showing the correlation between θ and (a) γ^P and (b) γ^T for all samples with a SigmaPlot Quadratic Dynamic Curve Fit.

TABLE 2
Results summary for all nylon 6,6 samples showing roughness parameters, surface oxygen content and wettability characteristics.

Sample ID	Sa (μm)	Ra (μm)	γ^P (mJm^{-2})	γ^D (mJm^{-2})	γ^T (mJm^{-2})	Surface Oxygen Content (%at.)	Contact Angle (°)
NAR	0.126	0.029	17.69	29.66	47.34	13.26±0.27	56.4±1.2
CT50	0.636	0.148	12.24	28.63	40.87	14.33±0.29	66.0±4.0
CT100	0.297	0.185	16.86	29.83	46.69	14.05±0.28	57.5±2.4
CH50	0.423	0.103	10.93	31.64	42.58	14.99±0.30	65.8±2.9
CH100	0.326	0.155	13.63	30.37	44.00	14.84±0.30	62.2±2.3

pattern (samples PT50 and PH50, respectively) allowing these samples to become more hydrophilic. In contrast, the 100 μm trench pattern (sample PT100) gave rise to a contact angle that was greater than that of the as-received sample (PAR) and can also be seen as hydrophobic since the contact angle was greater than 90°. It was also seen that the contact angle was equivalent to the as-received sample (PAR) for the 100 μm hatch patterned sample (PH100).

With regards to the 50 μm dimension patterned samples (PT50 and PH50) the reduction in contact angle could be seen to be a result of the increase in surface roughness, apparent polar component, γ^P, and increase in total apparent surface free energy, γ^T. This is concurrent with existing theory which states that for a hydrophilic material the contact angle should decrease upon an increase in surface roughness and apparent γ^P [25,38,39] Conversely, for the 100 μm trench and hatch patterned samples (PT100 and PH100) the contact angle was seen to increase even though the surface roughness and γ^T had increased considerably. This does not necessarily fit with previous works [25] as an increase in surface roughness and γ^T should bring about a reduction in θ. On account of this, it is possible that a mixed-state wetting regime [14,18] gave rise to these differences in results.

Table 1 also gives the XPS analysis data for surface oxygen content in order to detail any changes made during the laser processing. Through XPS analysis it was identified that the carbon content of each of the laser patterned PMMA samples decreased slightly, by up to 6 %at. compared to the as-received sample, PAR; whereas the oxygen content had increased slightly, by up to 5.5 %at. compared to the as-received sample, PAR. Owing to the data given in Table 1 it is possible to determine that a change in oxygen content alone, in this instance, does not necessarily give an explanation as to the variation in contact angles observed for the laser surface engineered PMMA samples. One possible explanation to the observation of significant variation in contact angle values is that of the dominant wetting regime present. For those PMMA samples with contact

angles less than that obtained for the as-received sample (PAR), it is highly likely that the Wenzel wetting regime is dominant in which the whole surface wets. For the laser patterned samples which had contact angles greater than that obtained for the as-received sample it is possible that either the Cassie-Baxter impregnation regime [40,41] was dominant or an intermediate mixed state was present. The Cassie-Baxter regime describes a droplet of water on a surface which gives rise to air gaps forming along the liquid-surface boundary. Whereas the Cassie-Baxter impregnation regime and intermediate mixed state, refers to a droplet of liquid on a surface in which both Wenzel and Cassie-Baxter regimes are present. It has been hypothesized previously that the mixed wetting state may be present when studying the wettability of laser patterned nylon 6,6 [42]; however, it is not conclusive in this instance and would require further investigation to determine if this was the case or not. As a result it is highly likely that the change in contact angle is dominated by the laser induced pattern to give rise to different wetting regimes. However, ultimately roughness and surface oxygen content cannot be dismissed as through further work it may be possible to ascertain whether these parameters, along with surface roughness and pattern, are contributing factors to the determination of the resulting contact angle. Further discussion of this is presented in Section 4.0.

Table 2 gives a summary of the results obtained for each of the laser surface engineered nylon 6,6 samples including surface roughness, wettability characteristics parameters, surface oxygen content and contact angle. As it has been stated previously, current theory states that for a hydrophilic material such as nylon 6,6 an increase in roughness and surface oxygen content should bring about a reduction in θ [25]. But, Table 2 shows that this was not the case for the CO_2 laser-induced patterned samples as θ had increased by up to 10° even though a maximum increase in Sa was determined to be around 0.5 μm when compared to the as-received sample (NAR). As hypothesized previously [43], this phenomenon can be explained by the existence of an intermediate wetting regime, such as Cassie-Baxter impregnation regime or a mixed-wetting state and will be further discussed later in Section 4.0. This mixed-state wetting regime can also account for the observed reduction in apparent γ^P and apparent γ^T with γ^P reducing by up to 8 mJm^{-2} and γ^T reducing by up to 7 mJm^{-2}, when compared to the as-received sample (NAR) which had γ^P and γ^T values of 17.69 and 47.34 mJm-2, respectively.

Comparing both the PMMA and nylon 6,6 samples together, it has been observed that current theory has not been corroborated with, in terms of the laser-induced patterning of nylon 6,6, insofar as the increase in Sa and Ra have not given rise to a reduction in θ. However, it has been seen that γ^T may have had a significant impact on the wetting nature of the PMMA and nylon 6,6, even if a wetting transition has taken place. Figure 9 shows the relation-

ship between θ and γ^P and γ^T. From these graphs it is possible to identify that by collating all results, for all samples studies, the laser-induced patterning of PMMA and nylon 6,6 gave rise to θ with a strong inverse function in correlation with γ^P and γ^T. On account of this, it is reasonable to say that for the laser surface engineered PMMA and laser engineered nylon 6,6 samples γ^P and γ^T were dominant parameters for determining the wettability characteristics of the polymeric materials.

Surface roughness and surface topography is another surface parameter which could have had a significant impact upon the way in which a material wets [3]. From Figure 10 it can be seen that the surface roughness in terms of Ra and Sa that there was some slight correlation between θ and the surface roughness, Sa (Figure 10(a)) and Ra (Figure 10(b)). This is owed to the fact that the tendency for all polymeric samples was to give rise to an increase in θ on account of the increase in laser surface engineered polymeric samples. This is significant as it could highlight that the laser surface engineering of the polymeric material, effectively inducing grooves in this case, impacted upon the droplet manipulation during the time of contact angle measurements, giving rise to specific wetting transitions as will be further discussed in Section 4.0. Having said that, it should be noted that the correlation of θ to Sa and Ra is not as strong when compared with γ^T and its polar component. This is owed to the fact that θ was erratic for certain samples, not showing a strong correlative trend, and could further indicate that the laser-induced grooved pattern had a major impact upon the liquid slippage across the sample. Further discussion of this is provided in Section 4.0. One other aspect to consider with surface roughness of laser surface engineered polymeric materials is that of the difference in melting temperature and stability of materials under melting. That is, with nylon 6,6 having a melting temperature higher than PMMA by 100°C it is more stable and as a result will be molten over a lesser period of time compared to the PMMA. On account of this, as the PMMA would have been molten for longer, there would likely have been more movement in the melt giving rise to a higher surface roughness.

As can be seen from Table 1, Table 2 and Figure 11, for all laser surface engineered samples, the surface oxygen content had increased which can be attributed to oxidation of the surface during the laser processing. By collating all of the resulting θ and considering the surface oxygen content for each sample (see Figure 11) it was possible to ascertain that there appeared to be a strong correlation between the resulting θ and the laser-induced increase in surface oxygen content for both of the polymeric materials. This correlates with the work of others who indicate that surface chemistry does play an important role in the determination of wetting transitions and wetting regimes for polymeric materials [5,44,45]. With this in mind, it is likely that both the laser-induced modifications of surface topography and surface chemistry of the two polymeric materials impacted upon the wetting transitions and the ultimate wetting regimes taking place on the surfaces of the samples.

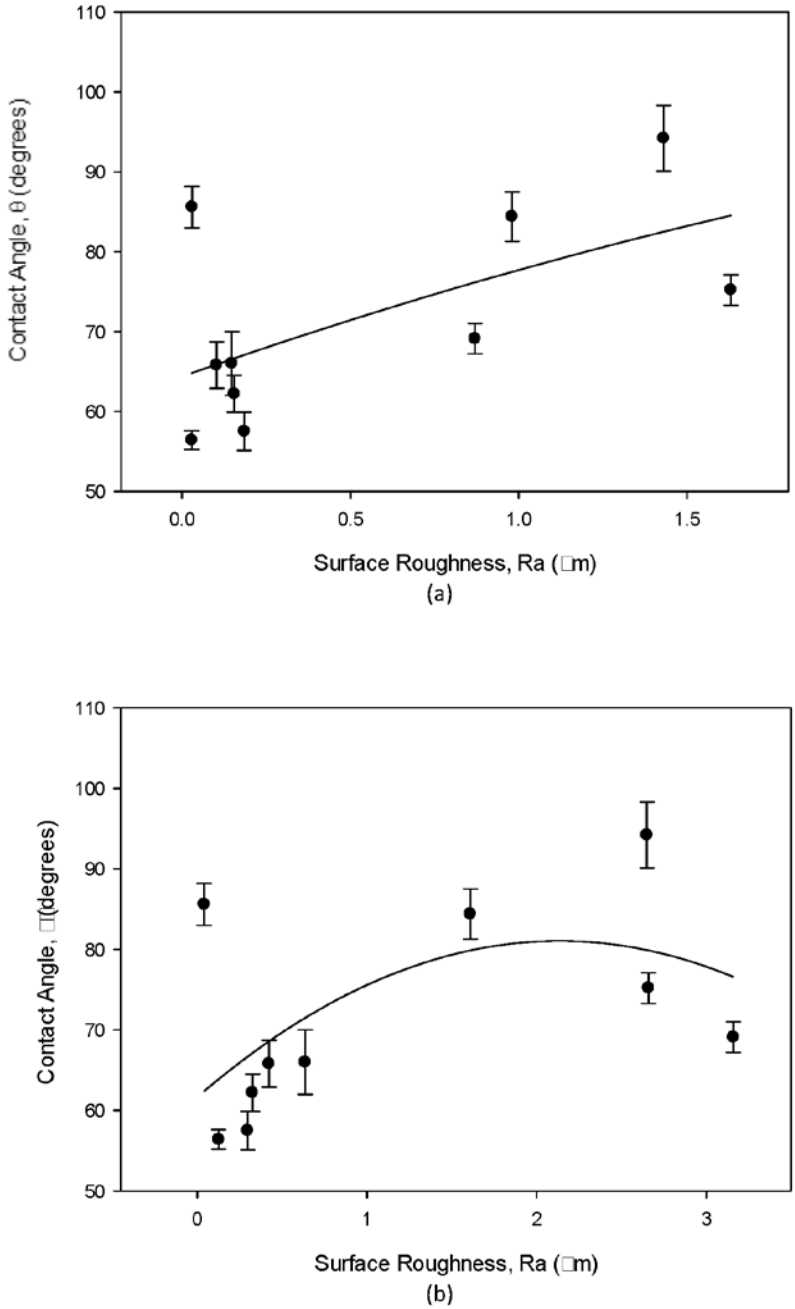

FIGURE 10
Graphs showing the correlation between θ, (a) Ra and (b) Sa for all samples with a SigmaPlot Quadratic Dynamic Curve Fit.

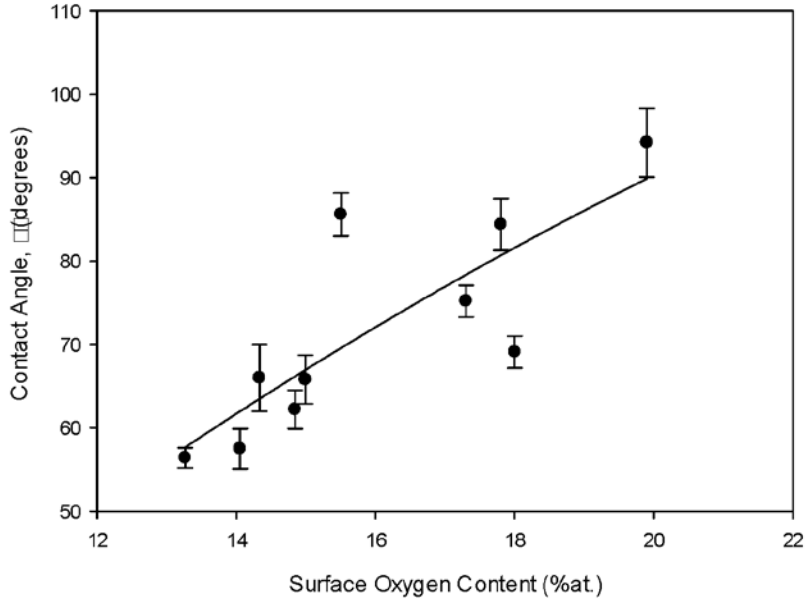

FIGURE 11
Graph showing the correlation between θ and the surface oxygen content for all samples with a SigmaPlot Quadratic Dynamic Curve Fit.

4 WETTING TRANSITIONS ON LASER SURFACE ENGINEERED POLYMERS

Even though there is still a considerable amount which is unknown about liquid-surface interfaces and the theories/hypotheses surrounding it, there has been significant developments over the last 15 years on the wetting behaviour of rough surfaces [18,40,41]. This has taken in to account aspects such as time to contact [12], energy paths [17], wetting transitions [46], external factors such as pressure and vibrations [18] and a deeper understanding and definition of various wetting states [40,41]. Another area of increased interest is that of the production of surfaces with stable wetting transitions and stable wetting regimes, especially in the field of omniphobic material applications [18].

A significant piece of work conducted by Lee et al. [12] described that liquid droplet impact and contact line velocity for the droplet incident on a rough surface is critical for influencing the wetting transitions taking place. This is highly noteworthy as they showed that these aspects can lead to the development of two different wetting transitions, having a notable effect on the liquid-surface interface. What is more, they discuss that the development of pressure and wetting area seem to significantly impact upon the resulting wetting transition and ultimately, the resulting wetting regime. With this in mind, it is imperative that all researchers keep this in mind when studying rough surfaces and

how they wet. This is owed to the fact that the impact and contact line velocity of a liquid droplet on a rough surface will influence the resulting wetting regime and the ability for wetting transitions to take place. As a result, this should be considered and discussed in all work relating to the wetting of rough surfaces, the wetting regimes taking place on those rough surfaces and the consideration of any wetting transitions which take place over that rough surface. In addition to this, Pashos et al. [17] described how grooved surfaces can give rise to localised drooping of the liquid droplet between the grooves, at a liquid-solid interface. They hypothesized that this could lead to localized wetting transitions across the grooved surface corresponding to discrete areas across grooves. With the laser surface engineered samples discussed in this work, in particular the laser surface patterned samples, this could be significant as the laser scanned lines gave rise to fluctuations of grooves across the polymeric surfaces. That being said, this could result in various wetting transitions across the surface giving rise to unexpected contact angle data. It may even be possible that the contact angle data identified for these surfaces results from a combination of the various wetting transitions over the laser surface engineered surface. This would likely have a large effect on the slipping nature of the droplet across the surface as it is well known, from the navier-slip model [12], that rough surfaces reduce slippage of liquids across a solid surface. This will ultimately effect the minimum energy paths of wetting transitions which can lead to intermediate or mixed-state wetting regimes [17,46]. Furthermore, as discussed by Bormashenko [18], hierarchical surfaces have a tendency to be less susceptible to wetting transitions and can be accounted for by the reduction in slippage. This may be the case with the laser surface engineered samples as there did appear to be a hierarchical surface roughness resulting from the laser surface processing.

How droplets of liquid on a solid surface react to external pressure has also been considered within the last seven years by Bormashenko [18,41]. This work showed how external pressure can significantly affect the wetting transitions on rough surfaces to the point where a critical pressure can be determined [18]. In addition to this, Bormashenko [18] states that the critical pressure value can be increased through the reduction of surface feature scales. Some initial studies regarding the impact of pressure on laser surface engineered polymeric materials has already been conducted [47]; however, considerably more work is required in this area to ascertain the impact of external forces on the wetting transition and wetting regimes of liquids on laser surface engineered polymeric materials. In addition to pressure, the impact of ambient temperature on the resulting contact angle has also been studied by Diaz et al. [48] showing that the temperature has some impact on the contact angle equilibrium. With this in mind, the ambient temperature when studying laser surface engineered materials and the subsequent effects on contact angle should be accounted for. Having said that, it has been noted that the temperature tends to play a small role in the definition of the contact angle equilibrium [48].

It has previously been hypothesized that the variation in contact angles on laser surface patterned polymeric materials arises from a transition from a Wenzel state to that of a mixed wetting regime state [19,20,43]. It should be noted that further work is required to establish whether this is the case or not. With this in mind, the Cassie impregnating wetting state [40,41] should also be considered as a potential wetting transition arising on laser surface engineered polymeric materials. In order to do this, the energy barrier, critical pressure and dimension of wetting transitions need to be accounted for with regards to the laser surface engineered polymeric materials.

5 SUMMARY

Through this study it has been demonstrated that following CO_2 laser surface engineering of PMMA and nylon 6,6 the surface characteristics can be modified in order to have influence over the contact angle. This has significant implications on the wetting and adhesion nature of the materials. What is more, it has been shown that it is highly likely that the laser-induced modification of topography and surface chemistry has a likely impact upon the resulting wetting transitions and wetting regimes pertaining to the modified surfaces. It was found that the surface roughness can be increased by up to an Sa of 3 μm and an Ra of 1.6 μm for PMMA and nylon 6,6 samples in comparison to the as-received samples which yielded an Sa of 0.04 μm for sample PAR and 0.126 μm for sample NAR. It was also observed that, as a result of the thermolytical interaction between the laser beam and the material, considerable melting and re-solidification took place. In some instances, this melting and re-solidification gave rise to the eradication of the natural periodicity of the laser induced pattern. This was especially seen for the 50 μm hatch samples as the beam scan of the pattern overlapped owed to the laser spot size incident on to the material being approximately 95 μm.

In terms of laser-modified wettability and contact angle of the PMMA and nylon 6,6, it was found that there was a strong inverse correlation between θ and γ^P and γ^T. Since, θ was found to be a strong correlative decreasing function of both γ^P and γ^T this identified that the apparent surface free energy played a major role in the determination of the wettability of nylon 6,6. With this in mind, it is reasonable to say that this result allows one to realize that the wettability of laser-modified nylon 6,6 could be predicted by knowing the apparent surface free energy and its components of the laser-induced roughened polymeric surface.

Furthermore, it was identified that there was some correlative trend between θ and the surface roughness and θ and the surface oxygen content. This is significant as, whilst current theory has not been adhered too such that an increase in surface roughness did not bring about a reduction

in θ, the correlative trends do show that the laser-modified surface parameters gave rise to a somewhat predictable θ. Based on the data observed within this work and from current understanding in the literature it seems highly likely that the laser-modified polymeric surfaces are giving rise to significant changes in wetting transitions, which is impacting upon the ultimate wetting regime taking place on the laser-modified polymeric surfaces. That being said, based on the available literature and current understanding of the wetting of rough surfaces, it is highly likely that for both PMMA and nylon 6,6 the Wenzel regime on the as-received samples is transitioning to either a Cassie-Baxter impregnation regime or an intermediate mixed-state wetting regime. This is on account of the laser surface engineering taking place giving rise to a surface which reduces droplet slippage on account of grooves being present on the laser surface engineered polymeric materials. It should be noted here, though, that further work is required to model such surfaces in order to ascertain the corresponding energy barriers for the laser surface engineered polymeric materials to gain a further, deeper understanding of the wetting transitions and wetting regimes taking place.

With an increase in industrial and academic interest in surface engineering and adhesion theory, the work conducted here has shown that laser technology can be effectively applied to elicit variations in a number of surface characteristics which results in a modulation of the wettability and adhesion characteristics. With this in mind, laser surface engineering can be seen to be a highly attractive means of simultaneously and discretely modifying the surface properties of materials and can be used to enhance these surface properties to optimize a material for specific applications such as bioengineering, electronics and coating technologies.

REFERENCES

[1] Kim T., Min C., Jung M., Lee J., Park C. and Kang S. Design methodology for nano-engineered surfaces to control adhesion: Application to the anti-adhesion of particles. *Applied Surface Science* **389** (2016), 889-893.

[2] Chang C. and Duh J. Duplex coating technique to improve the adhesion and tribological properties of CrAlSiN nanocomposite coating. *Surface and Coatings Technology* **326** (2016), 375-381.

[3] Mittal K.L. and Bahners T. *Laser Surface Modification and Adhesion.* Beverly, MA, USA: Wiley-Scrivener. 2015.

[4] Bayle M., Waugh D.G., Colston B.J. and Lawrence J. On the study of oil paint adhesion on optically transparent glass: Conservation of reverse paintings on glass. *Applied Surface Science* **357** (2015), 293-301.

[5] Pfleging W., Bruns M., Welle A. and Wilson S. Laser-assisted modification of polystyrene surfaces for cell culture applications. *Applied Surface Science* **253** (2007), 9177-9184.

[6] Mao C., Zhao W., Zhu C., Zhu A., Shen J. and Lin S. In vitro studies of platelet adhesion on UV radiation-treated nylon surface. *Carbohydrate Polymers* **59** (2005), 19-25.

[7] Riveiro A., Soto R., del Val J., Comesaña R., Boutinguiza M., Quintero F., Lusquinos F. and Pou J. Laser surface modification of ultra-high-molecular-weight polyethylene (UHMWPE) for biomedical applications. *Applied Surface Science* **302** (2014), 236-242.

[8] Waugh D.G. and Lawrence J. Laser Surface Processing of Polymers for Biomedical Applications. in: Majumdar J.D. and Manna I. (Eds.) *Laser-Assisted Fabrication of Materials.* Berlin, Germany: Springer Berlin Heidelberg. 2012. pp. 275-318.

[9] Gillett A., Waugh D.G., Lawrence J., Swainson M. and Dixon R. Laser surface modification for the prevention of biofouling by infection causing *Escherichia Coli. Journal of Laser Applications* **28** (2016) 022503.

[10] Telford A.M., Thickett S.C. and Neto C. Functional patterned coatings by thin polymer film dewetting. *Journal of Colloid and Interface Science* **507** (2017) 453-469.

[11] Janjua Z.A., Turnbull B., Choy K., Pandis C., Liu J., Hou X. and Choi K.S. Performance and durability tests of smart icephobic coatings to reduce ice adhesion. *Applied Surface Science* **407** (2017), 555-564.

[12] Lee C., Nam Y., Lastakowski H., Hur J., Shin S. and Biance A.L. Two types of Cassie-to-Wenzel wetting transitions on superhydrohobic surfaces during drop impact. *Soft Matter* **11** (2015), 4592-4599.

[13] Cardoso M.R., Tribuzi V., Balogh D.T., Misoguti L. and Mendonça C.R. Laser microstructuring for fabricating superhydrophobic polymeric surfaces. *Applied Surface Science* **257** (2011), 3281-3284.

[14] Waugh D.G. and Lawrence J. Wettability Characteristics of Laser Surface Engineered Polymers. in Mittal K.L. and Lei W.S. (Eds.) *Laser Technology: Applications in Adhesion and Related Area*. NJ, USA: Scrivener Publishing LLC, John Wiley & Sons, 2018. p. 99--122.

[15] Pashos G., Kokkoris G. and Boudouvis A.G. A modified phase-field method for the investigation of wetting transitions of droplets on patterned surfaces. *Journal of Computational Physics* **283** (2015), 258-270.

[16] Pant R., Singha S., Bandyopadhyay A. and Khare K. Investigation of static and dynamic wetting transitions of UV responsive tunable wetting surfaces. *Applied Surface Science* **292** (2014), 777-781.

[17] Pashos G, Kokkoris G, Boudouvis AG. Minimum Energy Paths of Wetting Transitions on Grooved Surfaces. Langmuir 2015;31:3059-3068.

[18] Bormashenko E. Progress in understanding wetting transitions on rough surfaces. *Advances in Colloid and Interface Science* **222** (2015), 92-103.

[19] Waugh D.G. and Lawrence J. Wettability characteristics variation of nylon 6,6 by means of CO2 laser generated surface patterns. *The 27th International Congress on Application of Lasers and Electro-Optics (ICALEO 2008)*, 10-24 October 2008, Temecula, CA., USA.

[20] Waugh D.G., Lawrence J. and Shukla P. Modulating the wettability characteristics and bioactivity of polymeric materials using laser surface treatment. *Journal of Laser Applications* **28** (2016), 022502.

[21] Patil A., Patel A. and Purohit R. An overview of polymeric materials for automotive applications. *Materials Today: Proceedings* **4** (2017), 3807-3815.

[22] Thomas M. and Mittal K.L. *Atmospheric Pressure Plasma Treatment of Polymers: Relevance to Adhesion*. Beverly, MA, USA: Wiley-Scrivener. 2013.

[23] Kiriy A,, Pötzsch R., Wei Q, and Voit B. High-tech functional polymers designed for applications in organic electronics. *Polymer Degradation and Stability* **145** (2017) 150-156.

[24] Waugh D.G. and Lawrence J. *Laser Surface Treatment of a Polymeric Biomaterial: Wettability Characteristics and Osteoblast Cell Response Modulation*. Philadelphia, USA: Old City Publishing. 2014.

[25] Hao L. and Lawrence J. *Laser Surface Treatment of Bio-Implant Materials*. New Jersey, USA: John Wiley & Sons Inc. 2005.

[26] Lai J., Sunderland B., Xue J., Yan S., Zhao W., Folkard M., Michael B.D. and Wang Y. Study on hydrophilicity of polymer surfaces improved by plasma treatment. *Applied Surface Science* **252** (2006), 3375-3379.

[27] Malinauskas M., Zukauskas A., Hasegawa S., Hayasaki Y., Mizeikis V., Buividas R. and Juodkazis S. Ultrafast laser processing of materials: from science to industry. *Light: Science and Applications* **5** (2016), e16133.

[28] Hecht J. *The Laser Guidebook: Second Edition*. NJ, USA: McGraw-Hill Inc.1992.

[29] Waugh D.G. and Lawrence J. *Laser surface engineering: Processes and Applications*. Cambridge, UK: Elsevier Ltd. 2015.

[30] Bacakova L., Filova E., Parizek M., Ruml T. and Svorcik V. Modulation of cell adhesion, proliferation and differentiation on materials designed for body implants. *Biotechnology Advances* 29 (2011), 739-767.

[31] See T.L., Liu Z., Li L. and Zhong X.L. A comparison of the characteristics of excimer and femtosecond laser ablation of acrylonitrile butadiene styrene (ABS). *Applied Surface Science* **364** (2016), 467-476.

[32] Mirzadeh H. and Dadsetan M. Influence of laser surface modifying of polyethylene terephthalate on fibroblast cell adhesion. *Radiation Physics and Chemistry* **67** (2003), 381-385.

[33] Wang Z.K., Zheng H.Y. and Lam Y.C. Investigation on femtosecond laser irradiation energy in inducing hydrophobic polymer surfaces. *Applied Surface Science* **257** (2011), 10427-10433.

[34] Sobac B. and Brutin D. Triple-line behavior and wettability controlled by nanocoated substrates: influence on sessile drop evaporation. *Langmuir* **27** (2011), 14999-15007.

[35] Ström G., Frederikson M. and Stenius P. Contact Angles, Work of Adhesion, and Interfacial Tensions at a Dissolving Hydrocarbon Surface. *Journal of Colloid and Interface Science* **119** (1987), 352-361.

[36] Żenkiewicz M. Methods for the calculation of surface free energy of solids. *Journal of Achievements in Materials and Manufacturing* **24** (2007), 137-145.

[37] Waugh D.G. and Lawrence J. Wettability and osteoblast cell response modulation through UV laser processing of nylon 6,6. *Applied Surface Science* **257** (2011), 8798-8812.

[38] Waugh D.G., Lawrence J., Brown E.M. Osteoblast cell response to a CO2 laser modified polymeric material. *Optics and Lasers in Engineering* **50** (2012), 236-247.

[39] Waugh D.G., Hussain I., Lawrence J., Smith G.C., Cosgrove D. and Toccaceli C. In vitro mesenchymal stem cell response to a CO2 laser modified polymeric material. *Materials Science and Engineering C* **67** (2016), 727-736.

[40] Ishino C., Okumura K. and Quéré D. Wetting transitions on rough surfaces. *EPL (Europhysics Letters)* **68** (2004), 419-425.

[41] Bormashenko E. Wetting transitions on biomimetic surfaces. Philosophical Transactions of the Royal Society of London A: *Mathematical, Physical and Engineering Sciences* **368** (2010), 4695-4711.

[42] Waugh D.G. and Lawrence J. CO2 laser surface patterning of nylon 6,6 and subsequent effects on wettability characteristics and apatite response. *Surface Engineering* **27** (2011), 724-728.

[43] Waugh D.G., Lawrence J., Walton C.D. and Zakaria R.B. On the effects of using CO2 and F2 lasers to modify the wettability of a polymeric biomaterial. *Optics & Laser Technology* **42** (2010), 347-356.

[44] Zhao Y., Tan K., Zhou Y., Ye Z. and Tan W. A combinatorial variation in surface chemistry and pore size of three-dimensional porous poly(ε-caprolactone) scaffolds modulates the behaviors of mesenchymal stem cells. *Materials Science and Engineering C* **59** (2016),193-202.

[45] Ponsonnet L., Comte V., Othmane A., Lagneau C., Charbonnier M., Lissac M. and Jaffrezic N. Effect of surface topography and chemistry on adhesion, orientation and growth of fibroblasts on nickel–titanium substrates. *Materials Science and Engineering C* **21** (2002), 157-165.

[46] Pashos G., Kokkoris G., Papathanasiou A.G. and Boudouvis A.G. Wetting transitions on patterned surfaces with diffuse interaction potentials embedded in a Young-Laplace formulation. *The Journal of Chemical Physics* **144** (2016), 034105.

[47] Waugh D.G., Lawrence J. and Morgan D.J. Investigation into time dependant degradation and atmospheric conditions on the wettability of nylon 6,6 which has undergone CO2 laser surface modification. *Proceedings of the International Congress on the Application of Lasers and Electro-Otpics* (2009), 98-108.

[48] Diaz M.E., Savage M.D. and Cerro R.L. The effect of temperature on contact angles and wetting transitions for n-alkanes on PTFE. *Journal of Colloid and Interface Science* **503** (2017), 159--167.